23rd IMEKO TC4 International Symposium
Electrical & Electronic Measurements Promote Industry 4.0
September 17-20, 2019，Xi'an, China

# Measurement Procedure for External Magnetic Field in UME Kibble Balance

H Ahmedov, B Korutlu, L Dorosinskiy, R Orhan

*TÜBİTAK National Metrology Institute (UME), Kocaeli, TURKEY, haji.ahmadov@tubitak.gov.tr*

***Abstract* – The kilogram, currently defined by the mass of a material artifact, the International Prototype of the Kilogram, will be defined in terms of a fundamental nature of constant, the Planck constant, ensuring long-term stability of the SI mass unit and enabling traceability from more than one source. Kibble balance experiments offer an effective primary realization method for the kilogram based on the value of Planck constant. Kibble Balance apparatus operating at National Metrology Institute of Turkey is designed with a stationary coil and an oscillating magnet. In contradistinction to traditional moving coil Kibble balance experiments, external magnetic field brings an asymmetry between the Ampere's law of force and the Faraday's law of induction in moving magnet experiments. In this paper, we develop a method based on the external magnetic flux density difference measurements in vertical direction to take into account the effect of the external magnetic field on the realization of kilogram. The proposed model in this approach fits well with the data such that the kilogram realization requirement is met within the accuracy of the measuring instrument.**

***Keywords – Kibble balance, magnetic flux density, measurement techniques, Planck constant***

## I. INTRODUCTION

The redefinition of the kilogram unit, approved at the 26th meeting of The General Conference on Weights and Measures (CGPM) held in November 2018, has replaced its artifact definition via the mass of International Prototype of the Kilogram (IPK) with the one based on a fixed numerical value of Planck constant [1]. Extensive studies are performed in several national metrology institutes (NMIs) across the world to ensure a smooth transition to the revised definition of kilogram. Currently, there are two independent primary methods for realizing the kilogram with an uncertainty of a few parts in $10^8$: Kibble balance [2-22] and X-ray-crystal density (XRCD) [23-28]. The content of this paper bears upon the Kibble balance principle. Originally devised at the National Physical Laboratory (NPL) by Brian Kibble in 1975 [29, 30], the Kibble balance relates the mechanical and the electrical powers where the electrical power is measured in terms of Planck constant by using two macroscopic quantum phenomena known as quantum Hall effect [31] and Josephson effect [32] for linking the macroscopic mass to the Planck constant. A number of Kibble balances with different geometries and experimental protocols have been constructed in various NMIs [2-22]. National Metrology Institute of Turkey (UME) has constructed a Kibble balance with a stationary coil suspended from the load cell of mass comparator and a surrounding oscillating magnetic circuit. The prominent features of UME Kibble balance manifest themselves in the adopted novel measurement procedure where the oscillating parameters are continuously averaged over the magnet oscillation half-cycles (See [33-36] for details of the adopted measurement procedure). As a result, the variations in magnetic field and temperature are suppressed which in turn enables the construction of both the magnetic circuit and the apparatus in smaller dimensions. The oscillatory motion of the magnetic circuit allows also simultaneous operation of weighing and moving phases (i.e., concurrent testing of Ampere's force law and Faraday's law of induction) which eliminates the need for precisely quantifying the variations in the environmental and experimental conditions between the two phases. In addition, the system does not require a fine adjustment between the magnetic center of the magnetic circuit and electric center of the coil. Instead, the misalignment is treated as a parameter contributing to the Faraday's Voltage across the ends of the coil generated due to the relative motion between the coil and magnetic circuit [35, 36]. Apart from its distinctive properties, there is an important difference between UME Kibble Balance and traditional two-phase, moving coil Kibble balances such that external magnetic field brings an asymmetry between the Ampere's law of force and Faraday's law of induction. In the present work, we develop a convenient approach for taking into account the effect of earth magnetic field on oscillating magnet Kibble balance. The approach warrants the desired uncertainties in the realization experiment within the accuracy of the measuring instrument.

## II. KIBBLE BALANCE PRINCIPLE

A closed type, radially symmetric magnetic circuit is

used in UME Kibble balance, as it was confirmed to be the most practical solution for Kibble balance experiments realizing the kilogram. Such a magnetic circuit is known to produce radial and up-down symmetric fields in the air gap [37]. The cross sectional view of the magnetic circuit is given in Fig. 1. In the experiment, a stationary coil suspended from the load cell of the mass comparator carrying an electrical current $J$ is immersed in the air gap of the oscillating magnetic circuit. The magnetic circuit oscillates in the direction of the gravitational acceleration. A soft-iron yoke is used to guide the generated magnetic flux density towards the coil volume while effectively shielding the coil from the effect of varying external magnetic flux density. However, the exposure of the yoke itself, a magnetically non-linear material, to the external magnetic flux density and to the magnetic flux density by the magnetic circuit gives rise to an additional magnetic flux density in the air gap, the latter of which is called the magnetization flux density. Therefore, special attention needs to be paid to the effect of yoke on total magnetic flux density in the air gap.

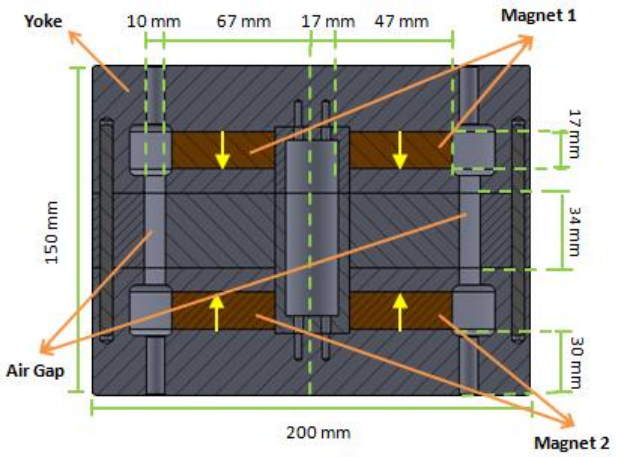


*Fig. 1. Cross-sectional view of the UME magnetic circuit. The yoke is made from iron and the permanent magnets from SmCo.*

Below we describe the asymmetry produced by the external magnetic field between Ampere's law of force and Faraday's law of induction:

*A. Ampere's Law of Force*

There are three sources of magnetic flux density created in the air gap

a) magnetic flux density generated by the magnetic circuit $(\vec{B}_{mc})$,
b) magnetization flux density ),
c) external magnetic flux density $(\vec{B}_e)$,

which contribute to the Ampere's force law given by where is the total magnetic flux density in the air gap and is the vector having a magnitude equal to the total length of the coil and being in the direction of electric current $J$. The Lorentz force on the coil in the direction of gravitational acceleration is obtained by the dot product where is the unit vector representing the direction of gravitational acceleration yielding

(1)

Here, $F_{mc}$ is the Lorentz force generated by the magnetic flux density of the magnetic circuit. $F_m$ and $F_e$ are the Lorentz forces induced on the coil by the magnetization and external magnetic flux densities, respectively. By using simple vector algebra, one may easily find that the Lorentz force is proportional to the magnetic flux through the lateral surface of the coil.

*B. Faraday's Law of Induction*

As the coil is stationary with respect to , only and contribute to the Faraday's law of induction. As a result, for an oscillating-magnet Kibble balance, the fundamental equation takes the following form

— — (2)

where V is a Faraday's voltage across the ends of the coil and u is the velocity of the coil with respect to the magnet. Using (2), the effect of external magnetic flux density on the Planck constant is found to be

— (3)

provided that the measurement procedure of the UME Kibble balance is followed [33, 34]. Here $\langle F_e \rangle$ and $\langle F$ are the mean values of the corresponding forces.

## III. THE MEASUREMENT PROCEDURE

Practically, the Lorentz force created by the external magnetic flux density is measured when there is no magnetic circuit. However, $q_m$ in (3) is proportional to the mean value of the Lorentz force on the coil generated by the external magnetic flux density during the experiment. Therefore, one needs to estimate the long term variations of this term. Using the fact that divergence of magnetic flux density over a closed surface is equal to zero, one may write the Lorentz force by the external magnetic flux as

——— (4)

where is the height of the coil, is the number of turns in the coil and is the flux difference between

top and bottom surfaces of the coil. The temporal changes in the flux through the coil may be characterized by using an additional nearby coil as the characteristic scales of the factors producing variations in external magnetic flux density is very large compared to the distance between the two coils. Therefore, one may relate the Lorentz force on the suspended coil from the load cell of the mass comparator to the magnetic flux difference through the auxiliary coil. In our measurement set-up we use magnetic flux gradiometer with the two vertically spaced magnetic sensors as auxiliary coil. As the output given by the gradiometer is magnetic flux density rather than the magnetic flux, we rewrite Eq. (4) in terms of the change in magnetic flux density $\delta B_e$ as follows

$$\frac{F_e(t)}{J} = \zeta\, \delta B_e(t), \tag{5}$$

where $\zeta$ is a model parameter which depends on the geometry of both coils and also on the local inhomogenities in the magnetic flux density which is found by minimization of the quadratic form

$$\mathfrak{F}(\zeta) = D\left(\frac{F_e}{J} - \zeta\, \delta B_e\right), \tag{6}$$

where $D$ is the standard deviation. Since the target accuracy in the realization of kilogram is twenty parts per billion, the modeling (5) will meet the requirements provided that

$$\sqrt{\mathfrak{F}}\,/\langle F\rangle < 10^{-8}. \tag{7}$$

## IV. MEASUREMENTS

The schematic circuit diagram of the measurement set-up for external magnetic field density measurements and the photo of UME Kibble Balance apparatus are given in Fig. 2 and Fig. 3, respectively.

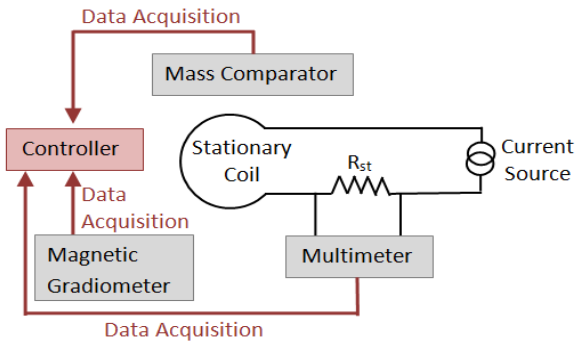


*Fig. 2. The schematic circuit diagram of the external magnetic flux density measurement procedure.*

*Fig. 3. The photo of UME Kibble Balance apparatus.*

It is important to emphasize that there is no magnetic circuit surrounding the coil in external magnetic flux density measurements. Therefore, the Lorentz force in (1) reduces to $F = F_e$. The force measurements are carried out with the load cell of AX5006 mass comparator with 1 μg resolution which is integrated to UME Kibble Balance. DC current is measured by Keysight 3458 A digital multimeter across the two Tinsley 5658A 100 Ω standard resistors connected in parallel and placed in oil bath. DC calibration of Keysight 3458 A digital multimeter with Programmable Josephson Voltage Standard (PJVS) yields an accuracy of 0.1 ppm. The uncertainty components in the force, standard resistance and the change in magnetic flux density measurements are small compared to the uncertainty due to the digital multimeter. Therefore, the total uncertainty is restricted by the uncertainty in DC voltage measurements. Fig. 4. illustrates the ratio of the force by external magnetic flux density $F_e$ and the DC current $J$ averaged in every 10 min. There is 10 min delay between each consecutive data. The current direction has been reversed in every 100 s for handling the drifts in the balance. We obtain the mean value of the ratio as $\langle F_e/J\rangle = -0.295$ mN/A and the standard deviation as $\sigma(F_e/J) = 0.005$ mN/A. Since the geometrical factor $\langle F/J\rangle$ in our experiment is about 150 N/A, using (3), we obtain $q_m = 1.97 \times 10^{-6}$ with a standard deviation of $3 \times 10^{-8}$. It is not possible to state the origin of such small deviations as our current measurement capacity is limited with the 0.1 ppm accuracy of electrical measurements.

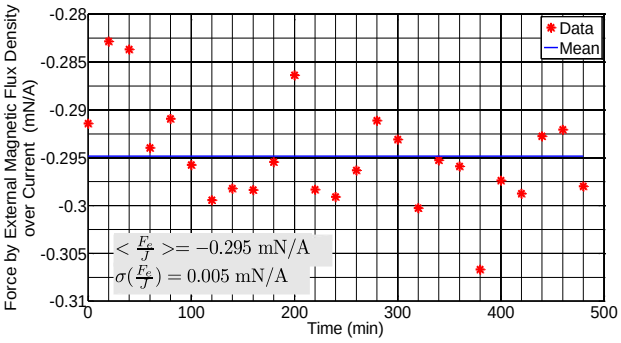


*Fig. 4. The ratio of the force by external magnetic flux density and DC current averaged in every 10 min. There is 10 min delay between each consecutive data. The current direction has been reversed in every 100 s for handling the drifts in the balance. The blue line indicates the mean value of the ratio. Numerical values of the mean and standard deviation are shown on the lower left corner of the graph.*

We use commercial Bartington single axis, vertical component fluxgate gradiometer for flux density difference measurements where two cylindrical gradiometer sensors are mounted on a rigid beam. Fig. 5. demonstrates the temporal changes in the difference of external magnetic flux density between the two sensors of the fluxgate gradiometer averaged in every 10 min. There is 10 min delay between each consecutive data.

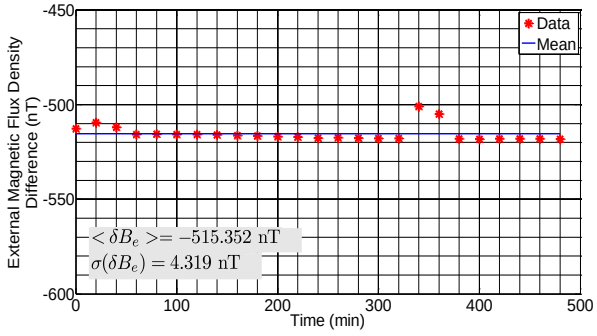


*Fig. 5. The temporal changes of the difference of external magnetic flux density between the two sensors of the fluxgate gradiometer averaged in every 10 min. There is 10 min delay between each consecutive data. The blue line indicates the mean value of the difference. Numerical values of the mean and standard deviation are shown on the lower left corner of the graph.*

The mean value of the temporal changes of external magnetic flux density between the two sensors is $\langle \delta B_e \rangle = -515.352$ nT and the standard deviation is $\sigma\langle \delta B_e \rangle = -4.319$ nT. The short term variations of the external magnetic flux density difference between the two sensors of fluxgate gradiometer are so small that it is not possible to monitor the Lorentz force temporal variations within the resolution of the mass comparator.

A pair of identical square coils of side length of 1.5 m separated at a distance equal to the side length of the square is introduced to create an additional axial magnetic flux density, $B_{axial}$, for producing short term variations of sufficient magnitude. A magnetic flux density of 1 Gauss is produced at the center of the coil pair provided that they are connected in series. The coil is placed next to the UME Kibble Balance apparatus. For our purposes, $I = 4$ A is switched on and off for every 10 min to create this additional flux density where $B_{axial} = 0$ is equivalent to case of coil being under the sole influence of external magnetic flux density. In Fig. 6 we show the temporal changes of the difference of magnetic flux density averaged in every 10 min in the presence and absence of the axial flux density. It is clear from Fig. 6 that there is an apparent difference in the external magnetic flux density in the presence (lower data) and in the absence of the axial field (upper data) which allows the Lorentz force measurements to be monitored with the mass comparator.

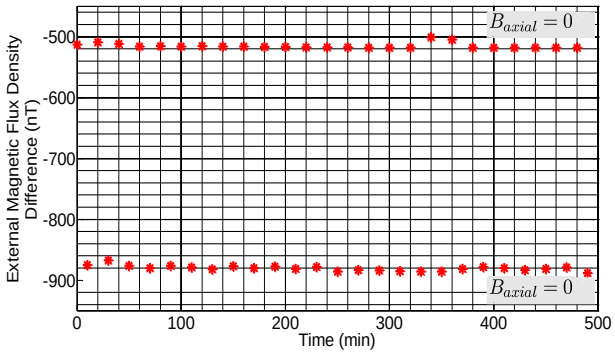


*Fig. 6. The temporal changes of the external magnetic flux density difference averaged in every 10 min when the axial field is on and off.*

With this data at hand, we solve for the optimization parameter $\zeta$ by minimizing the quadratic form in (6) which yields $\zeta = 583.7$ m. The actual data and model fitted data of the ratio $F_e(t)/J$ are given in Fig. 7. Given in red star is the actual data and in blue circles is the model fitting data with $\zeta = 583.7$ m. The actual data and fitted data coincide with each other. The target accuracy in (7) is achieved since we obtain $\sqrt{\mathfrak{F}}/\langle F \rangle = 4 \times 10^{-9}$.

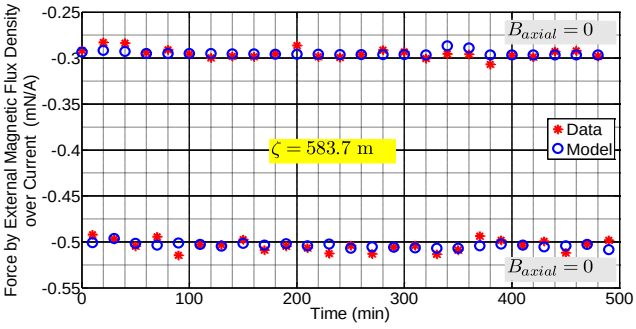


*Fig. 7. Fitting of the data by minimization of the quadratic form in (6). Given in red star is the actual data and in blue circles is the model fitting data with $\zeta = 583.7$ m.*

Since the effect of external magnetic flux on Planck constant is determined in the absence of the magnetic circuit, it is important to make the possible non-linear effects generated in the presence of the magnetic circuit negligible. The non-linear effects include the influence of the magnetic circuit on the nearby soft magnetic materials which in turn is reflected on the external magnetic flux. This could be achieved by keeping the magnetic materials away from the permanent magnet. The simulations are carried out in the EMS Magnetic Software to support this idea (see Fig. 8).

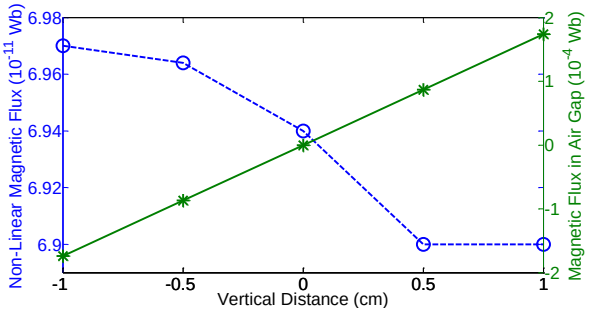


*Fig. 8. The simulation carried out in the EMS Magnetic Software. Given in blue dashed line with circle markers are the non-linear effect of external magnetic field and in green solid line with star markers indicate the magnetic flux in the air gap.*

We simulated the non-linear effect of external magnetic flux by using ferromagnetic material of cylindrical form with a diameter of 20 cm and height of 10 cm. The distance between the center of the ferromagnetic material and the magnetic circuit is taken to be 62.5 cm. The center of the ferromagnetic material is placed on the same symmetry axis with the magnetic circuit. We use pure iron as ferromagnetic materials The magnetic circuit oscillates vertically around the center of the coil with amplitude of 1 mm. The vertical distance given in the x-axis of Fig. 8 represents the distance between the center of the magnetic circuit and the center of the coil. As the height of the coil is around $d$ =2 cm, we simulated the region within a displacement of $\pm 1$ cm from the origin where the two centers coincide. The flux through the horizontal disk with the radius of 7 cm is simulated. The y-axis on the right represents the flux in the air gap for vertical displacements of $\pm 1$ cm from the origin while the one on the left represent the differences between the flux in the presence and in the absence of ferromagnetic material. The effect of non-linear flux is estimated to be $3 \times 10^{-9}$. It is important to note that in the actual experiment we expect the non-linear effects to be much smaller as there are no such heavy ferromagnetic materials nearby the magnetic circuit. In addition, magnetic circuit may directly affect the gradiometer sensors such that in the presence of magnetic circuit an offset $\delta B_{offset}$ will occur. However, it is possible to determine this offset independently by measuring the difference in the presence and absence of the magnetic circuit. Then, $\delta B_e$ would be replaced with $\delta B_e + \delta B_{offset}$ in the optimization procedure.

The asymmetry between Faraday's Law and Amperes Law can be treated with compensating coil as proposed by NIM Joule Balance Group [38]. In our system we are planning use both the compensating coil and the proposed magnetic gradiometer method to increase the reliability of the results. The comparative analysis between these two methods will be conducted after the ongoing modifications on the handler is complete.

## V. CONCLUSION

To deal with the impact of the external magnetic flux density on the Planck constant measurements we have proposed an approach based on vertical external magnetic flux density difference measurements. The model fitting the data meets the requirement for the realization of kilogram though the accuracy of the measurements is restricted by the equipment PJVS has been used in the calibration of the 3458A Digital Multimeter and 0.1 ppm accuracy is obtained. The current accuracy (0.1 ppm) in DC voltage measurements will be improved by using differential measurements after integrating PJVS to the measurement set-up [39].

## VI. ACKNOWLEDGMENT

This research is funded by TÜBİTAK National Metrology Institute of Turkey.

## REFERENCES

[1] Milton, M.J., Davis, R and Fletcher, N, *Towards a new SI: a review of progress made since 2011*, Metrologia, vol. 51, 2014, pp. R21–30.

[2] Robinson, I.A. and Kibble, B.P., *An initial measurement of Planck's constant using the NPL mark II watt balance*, Metrologia, vol. 44, 2007, pp. 427–40.

[3] Robinson, I.A., *Towards the redefinition of the kilogram: a measurement of the Planck constant using the NPL Mark II watt balance*, Metrologia, vol. 40, 2012, pp. 113-156.

[4] Inglis, A.D., Sanchez, C.A. and Wood, B.M., *The NRC watt balance project*, Digest 2010 Conf. on Precision Electromagnetic Measurements (Daejeon, Korea), 2010, pp. 514–5.

[5] Sanchez, C.A., Wood, B.M., Green, R.G., Liard, J. O. and Inglis, D, *A determination of Planck's constant using the NRC watt balance*, Metrologia, vol. 51, 2014, pp. S5-S14,.

[6] Steiner, R, Newell, D and Williams E, *Details of the 1998 Watt balance experiment determining the Planck constant*, J. Res. Nat. Inst. Stand. Technol., vol. 110, 2005, pp. 1–26.

[7] Schlamminger, S. et al., *A summary of the Planck constant measurements using a watt balance with a superconducting solenoid at NIST*, Metrologia, vol. 52, 2015, pp. L5-L8.

[8] Schlamminger, S. et al., *Determination of the Planck constant using a watt balance with a superconducting*

*magnet system at the National Institute of Standards and Technology*, Metrologia, vol. 51, 2014, pp. S15–24

[9] Haddad, D., et al., *A precise instrument to determine the Planck constant, and the future kilogram*, Rev. Sci. Instrum. vol. 87, 2016, pp. 061301.

[10] Baumann, H. et al, *Design of the new METAS watt balance experiment Mark II*, Metrologia, vol. 50, 2014, pp. 235–242.

[11] Geneves, G. et al., *The BNM watt balance project*, IEEE Trans. Instrum. Meas., vol. 54, 2005, pp. 850–3.

[12] Eichenberger, A, Geneves, G, and Gournay, P, *Determination of the Planck constant by means of a watt balance*, Eur. Phys. J. Spec. Top., vol. 172, 2009, pp. 363–83.

[13] Sutton, C.M., *An oscillatory dynamic mode for a watt balance*, Metrologia, vol. 46, 2009, pp. 467–72.

[14] Sutton C.M. et al., *A magnet system for the MSL watt balance*, Metrologia, vol. 51, 2014, pp. S101–6.

[15] Kim, D. et al., *Design of the KRISS watt balance*, Metrologia, vol. 51, 2014, pp. S96-100.

[16] Thomas, M. et al., *First determination of the Planck constant using the LNE watt balance*, Metrologia, vol. 52, 2014, pp. 433-43.

[17] Thomas, M. et al., *A determination of the Planck constant using the LNE Kibble balance in air*, Metrologia, vol. 54, 2017, pp. 468-80.

[18] Fang, H. et al, *Status of the BIPM watt balance*, IEEE Trans. Instrum. Meas., vol. 62, 2013, pp. 1491–8.

[19] Li, S. et al., *Coil-current effect in Kibble balances: analysis, measurement, and optimization*, Metrologia, vol. 55, 2018, pp. 75-83.

[20] Zhonghua, Z. et al., *The joule balance in NIM of China*, Metrologia, vol. 51, 2014, pp. S25-31.

[21] Zhengkun, L. et al., *The first determination of the Planck constant with the joule balance NIM-2*, Metrologia, vol. 54, 2017, pp. 763-74.

[22] Robinson, I.A. and Schlamminger, S, *The watt or Kibble balance: a technique for implementing the New SI definition of the unit of mass*, Metrologia, vol. 53, 2016, pp. A46 – A74.

[23] Andreas, B. et al., *Determination of the Avogadro constant by counting the atoms in a 28Si crystal*, Phys. Rev. Lett., vol. 106, 2011, pp. 030801.

[24] Andreas, B. et al., *Counting the atoms in a 28Si crystal for a new kilogram definition*, Metrologia, vol. 48, 2011, pp. S1–13.

[25] Azuma, Y. et al., *Improved measurement results for the Avogadro constant using a 28Si-enriched crystal*, Metrologia, vol. 52, 2015, pp. 360–75.

[26] Mana G. et al., *The correlation of the NA measurements by counting 28Si atoms*, J. Phys. Chem. Ref. Data, vol. 44, 2015, pp. 031209.

[27] Fujii, K, et al, *Realization of the kilogram by the XRCD method*, Metrologia, vol. 53, 2016, pp. A19-45.

[28] Kuramoto, N. et al., *Determination of the Avogadro constant by the XRCD method using a 28Si-enriched sphere*, Metrologia, vol. 54, 2017, pp. 716-29.

[29] Kibble, B.P., *A Measurement of the gyromagnetic ratio of the proton by the strong field method*, Atomic Masses and Fundamental Constants, vol. 5, ed. J. H. Sanders and A. H. Wapstra (New York: Plenum), 1976, pp 545–51.

[30] Kibble, B.P. and Robinson, I.A., *Feasibility study for a moving coil apparatus to relate the electrical and mechanical SI units*, Technical Report DES vol. 40, NPL, 1977.

[31] von Klitzing, K, Dorda, G and Pepper, M, *New method for high-accuracy determination of the fine-structure constant based on quantized Hall resistance*, Phys. Rev. Lett. vol. 45, 1980, pp. 494–7.

[32] Josephson, B.D., *Possible new effects in superconductive tunneling*, Phys. Lett. vol. 1 , 1962, pp. 251–3.

[33] Ahmedov, H, *An Oscillating magnet watt balance*, CPEM 2016 Conf. Digest, July 2016.

[34] Ahmedov, H, Babayiğit Aşkın, N, Korutlu, B and Orhan, R, *Preliminary Planck constant measurements via UME oscillating - magnet Kibble balance*, Metrologia, vol. 55, 2018, pp. 326-333.

[35] Ahmedov, H, Korutlu B and Orhan, R, *Optimization Procedure for Faraday's Voltage in UME Kibble Balance*, Digest 2018 Conf. on Precision Electromagnetic Measurements (Paris, France), 2018.

[36] Ahmedov, H, Korutlu, B and Orhan, R, *Optimization Procedure for Faraday's Voltage in UME Kibble Balance*, IEEE Transactions on Instrumentation and Measurement, vol. 68, no. 6, 2019, pp. 2172-2175.

[37] Schlamminger, S, *Design of the Permanent-Magnet System for NIST-4*, IEEE Trans. Instrum. Meas., vol. 62, 2012, pp. 1524 – 1530.

[38] Zhang, Z., et al., *Coils and the Electromagnet Used in the Joule Balance at the NIM*, IEEE Trans. Instrum. Meas., vol. 64, 2015, pp. 1539 – 1545.

[39] Behr, R *et al*., *Application of Josephson series arrays to a DC quantum voltmeter*, in IEEE Transactions on Instrumentation and Measurement, vol. 50, no. 2, 2001, pp. 185-187.